Eur. Phys. J. A **13**, 477–491 (2002)
DOI 10.1140/epja/iepja1357

THE EUROPEAN PHYSICAL JOURNAL A

Weak decays of heavy mesons in a covariant quark model

D. Merten[a], R. Ricken, M. Koll, B. Metsch, and H.R. Petry

Institut für Theoretische Kernphysik, Nußallee 14–16, D-53115 Bonn, Germany

Received: 19 December 2001 / Revised version: 17 January 2002
Communicated by V.V. Anisovich

Abstract. In this paper we investigate weak decays of heavy mesons in the framework of a covariant quark model, which is based on the Bethe-Salpeter equation in instantaneous approximation. Apart from a phenomenological confinement potential, a residual interaction induced by instantons is adopted. Masses and many decay observables of light mesons have already been described successfully in this model (Eur. Phys. J. A **9**, 73 (2000); 221). An appropriate extension allows a unified description of light and heavy systems. Using a set of parameters, which are fixed by the mass spectra, we evaluate the form factors of semileptonic decays of charmed and bottom mesons. In the heavy-quark limit these can be reduced to the Isgur-Wise function, which is calculated. Finally, the form factors are used to determine the non-leptonic decay rates of B-mesons in the factorization approximation.

PACS. 12.39.Ki Covariant quark model – 13.20.Fc Heavy mesons – 13.20.He Semileptonic decays

1 Introduction

In the last few years new and improved data on the spectra and the decays of charmed and bottom mesons have become available. The observations of the D_1^* and the radial excited $D^{*\prime}$ and B' have been published recently (see [1] and references therein). The dominant semileptonic decays of B, D and D_s mesons have been measured with good precision in the meantime, and data for double Cabibbo-suppressed channels are also available. Yet many new results will be provided by the B-factories BABAR, BELLE, HERA-B and LHC-B within the next years.

For the theoretical description of these masses and decays various ansätze are pursued. Lattice gauge theory gives good results for the transition form factors for high momentum transfer q^2, while QCD sum rules are suitable for the low-q^2 regime. Heavy-quark effective theory (HQET), which is based on a systematic expansion in the inverse mass of the heavy quark, provides some model-independent predictions, *i.e.* approximate degenerated mass doublets according to different orientation of the heavy-quark spin, and a connection between the semileptonic partial decay rate of the pseudoscalar and pseudovector decay channels, which has been experimentally confirmed. Unfortunately it cannot predict the masses and decay rates itself, and corrections due to the finite quark mass, at least for the charm quark, are expected to be substantial. Hence, for a consistent description of meson masses and decays over the full kinematic region, constituent quark models, even if the connection to the underlying theory is not quite clear, are still the most successful tool.

In previous papers, we have developed a relativistic constituent quark model for light mesons, which is based on the Bethe-Salpeter equation in instantaneous approximation. Apart from a phenomenological confinement potential we adopt a residual interaction induced by instantons. In this model, a very good description of the light-meson masses, from the ground state nonet up to highest angular momenta, has been achieved. Also many decay observables have been calculated in reasonable agreement with the experimental data (see [2] for a recent update). Motivated by this success, the model has been extended for heavy flavours [3]. Thereto we do not apply the one-gluon exchange, which is known to give a good description of heavy quarkonia and even of the whole meson spectrum with a suitable inclusion of relativistic effects [4]. Instead, we generalize the instanton-induced interaction in a naive way[1]. This is done in order to keep the model simple and unified: the parametrization of confinement should be valid for all flavours, and only one residual interaction is introduced. Also the question should be raised, when and how the model for light mesons fails, if higher quark and meson masses are involved. It turns out, that heavy-light mesons and, to a certain extent, heavy quarkonia can be described in that way. The resulting spectra together with a brief review of our model are discussed in sect. 2. Knowing the meson amplitudes we then calculate the semileptonic decays without further parameters in sect. 3. This

[a] e-mail: merten@itkp.uni-bonn.de

[1] For a similar investigation of weak meson decays in the Bethe-Salpeter framework with the one-gluon exchange see [5].

is done in order to test these amplitudes rather than to determine decay rates or CKM matrix elements with high precision. Therefore, we concentrate on the dominant processes $B \to D^{(*)}\ell\bar{\nu}$ and on the CKM-favoured decay channels of D and D_s mesons. Finally, in sect. 4 we investigate non-leptonic decays of B-mesons, and sect. 5 contains our summary.

2 The Bethe-Salpeter model

Since the model has been described earlier in greater detail [6,7], we will only briefly review the main features. The model is based on the Bethe-Salpeter equation for $q\bar{q}$ bound states

$$\chi^P(p) = -i\, S_1^F\left(\frac{P}{2}+p\right) \times \int\frac{\mathrm{d}^4p'}{(2\pi)^4}K(P;p,p')\chi^P(p')S_2^F\left(-\frac{P}{2}+p'\right), \quad (1)$$

for the Bethe-Salpeter amplitude

$$\chi^P(p) := \langle 0|T\psi(p)\bar{\psi}(p)|P\rangle.$$

Here $|P\rangle$ denotes a bound state with mass M and total momentum P, $P^2 = M^2$. In our ansatz the full quark propagators S_i^F are approximated by free fermion propagators $S_i^F(p) \approx i/(\not{p} - m_i + i\varepsilon)$, where the constituent quark masses m_i are introduced, which are treated as free parameters of the model. Furthermore, the irreducible interaction kernel K is assumed to be instantaneous in the rest frame of the meson, $K(P;p,p')|_{P=(M,\mathbf{0})} = V(\mathbf{p},\mathbf{p}')$. These assumptions lead to the (full) Salpeter equation

$$\Phi(\mathbf{p}) = \Lambda_1^-(\mathbf{p})\gamma^0\left[\int\frac{\mathrm{d}^3p'}{(2\pi)^3}\frac{V(\mathbf{p},\mathbf{p}')\Phi(\mathbf{p}')}{M+\omega_1+\omega_2}\right]\gamma^0\Lambda_2^+(-\mathbf{p}) - \Lambda_1^+(\mathbf{p})\gamma^0\left[\int\frac{\mathrm{d}^3p'}{(2\pi)^3}\frac{V(\mathbf{p},\mathbf{p}')\Phi(\mathbf{p}')}{M-\omega_1-\omega_2}\right]\gamma^0\Lambda_2^-(-\mathbf{p}) \quad (2)$$

for the Salpeter amplitude $\Phi(\mathbf{p}) := \int\frac{\mathrm{d}p^0}{2\pi}\chi^P(p)|_{P=(M,\mathbf{0})}$. Here $\omega_i := \sqrt{\mathbf{p}^2+m_i^2}$ and $\Lambda^\pm$ denotes the projector on positive and negative energy solutions of the Dirac equation. For the calculation of the meson mass M and the Salpeter amplitude Φ the Salpeter equation can be reformulated to an eigen value equation, which is solved numerically. This procedure is discussed in detail in [6,7]. We briefly sketch the numerical method in appendix A.

As ansatz for the interaction kernel we apply the sum of a phenomenologically motivated confinement potential and a residual interaction, which is induced by instantons. Confinement is parametrized by a linearly rising potential in configuration space with an adequate Dirac structure, symbolically written as

$$V_C(r) = (a_c + b_c\cdot r)\;\Gamma\otimes\Gamma.$$

To estimate the influence of the Dirac structure, two possibilities are taken into account, in the following referred to as model $\mathcal{A}$ and model $\mathcal{B}$: a combination of scalar and time-like vector, which has already been discussed in [6,7] and which is known to minimize spin-orbit splittings, and a chirally invariant combination of scalar, pseudoscalar and vector type, previously investigated by [8] and [9].

The additional instanton-induced residual interaction is based on the work of 't Hooft [10] and Shifman *et al.* [11]. The effect of QCD instantons on the quarks leads to an effective two-body interaction, which can be expressed by the following kernel in momentum space:

$$\int\frac{\mathrm{d}^3p'}{(2\pi)^3}V_{\mathrm{III}}(\mathbf{p},\mathbf{p}')\Phi(\mathbf{p}') = 4\,G\int\frac{\mathrm{d}^3p'}{(2\pi)^3}R_\Lambda(\mathbf{p},\mathbf{p}') \times\left(\mathrm{tr}\left[\mathbb{1}\Phi(\mathbf{p}')\right]\mathbb{1} + \mathrm{tr}\left[\gamma^5\Phi(\mathbf{p}')\right]\gamma^5\right). \quad (3)$$

The strengths of the coupling are collected in the flavour coupling matrix

$$G_{f_2f_3,f_1f_4} = \begin{cases} -g_{f_1f_2} : f_1 = f_3 \neq f_2 = f_4\,, \\ g_{f_1f_3} : f_1 = f_2 \neq f_3 = f_4\,, \\ 0 : \text{otherwise}, \end{cases} \quad (4)$$

with flavour indices f_i. The originally point-like interaction is regularized by the function R_Λ, for which a Gaussian form is used.

Heavy mesons have been included in this model to achieve a unified description of all mesons. Especially the parametrization of confinement should be universal. As shown in [3], this is done most successfully by extending the instanton-induced residual interaction in a naive way for heavy-light systems. This is done at the level of the interaction kernel eq. (3) by simply allowing $f_i \in \{u,d,s,c,b\}$ in (4). It has to be stressed that this extension is purely phenomenologically motivated, since the derivation leading to (3) is strictly valid for light quarks only. Also it should be mentioned that this use of the instanton-induced interaction allows the mixing of heavy and light flavours in the scalar and pseudoscalar flavour-neutral sectors. This has been investigated in [3] but will be neglected in this paper, since the effect turned out to be very small.

Due to the $J = 0$ selection rule of the residual interaction, a gradual fit of the model parameters to the light-meson masses has been performed as explained in [2], leading to the parameter sets in table 1. The resulting spectra of the isovector mesons are shown in fig. 1. The Regge trajectory is reproduced excellently in both models. The spectra of the light isoscalars and kaons are of similar quality. In particular the position of η and η' can be accounted for. The most significant difference between model $\mathcal{A}$ and $\mathcal{B}$ are the masses of the scalar mesons, *especially* the $a_0(980)$ in fig. 1. For a detailed discussion of these spectra we refer to [2] and [12].

Based on this parameter set the masses of the heavy quarks have been adjusted to the $J \neq 0$ heavy mesons. Finally, the additional couplings $g_{f_if_j}$ have been adjusted to reproduce the heavy-light pseudoscalar masses. We want to stress that in this way all heavy mesons except for the pseudoscalar D, D_s, B and B_s are described by fitting the heavy-quark masses only. The resulting spectra are

Table 1. The parameters of the confinement force, the 't Hooft interaction and the constituent quark masses in models $\mathcal{A}$ and $\mathcal{B}$.

	Parameter	Model $\mathcal{A}$	Model $\mathcal{B}$
Constituent quark masses	m_n (MeV)	306	380
	m_s (MeV)	503	550
	m_c (MeV)	1835	1780
	m_b (MeV)	5240	5092
Residual interaction	g_{nn} (GeV^{-2})	1.73	1.62
	g_{ns} (GeV^{-2})	1.54	1.35
	g_{nc} (GeV^{-2})	1.11	1.58
	g_{nb} (GeV^{-2})	0.53	1.07
	g_{sc} (GeV^{-2})	0.65	1.27
	g_{sb} (GeV^{-2})	0.00	0.76
	Λ (fm)	0.30	0.42
Confinement parameters	a_c (GeV)	−1.751	−1.135
	b_c ($\mathrm{GeV\ fm}^{-1}$)	2.076	1.300
Spin structure	$\Gamma \otimes \Gamma$	$\frac{1}{2}\left(\mathbb{1}\otimes\mathbb{1} - \gamma^0\otimes\gamma^0\right)$	$\frac{1}{2}\left(\mathbb{1}\otimes\mathbb{1} - \gamma^5\otimes\gamma^5 - \gamma_\mu\otimes\gamma^\mu\right)$

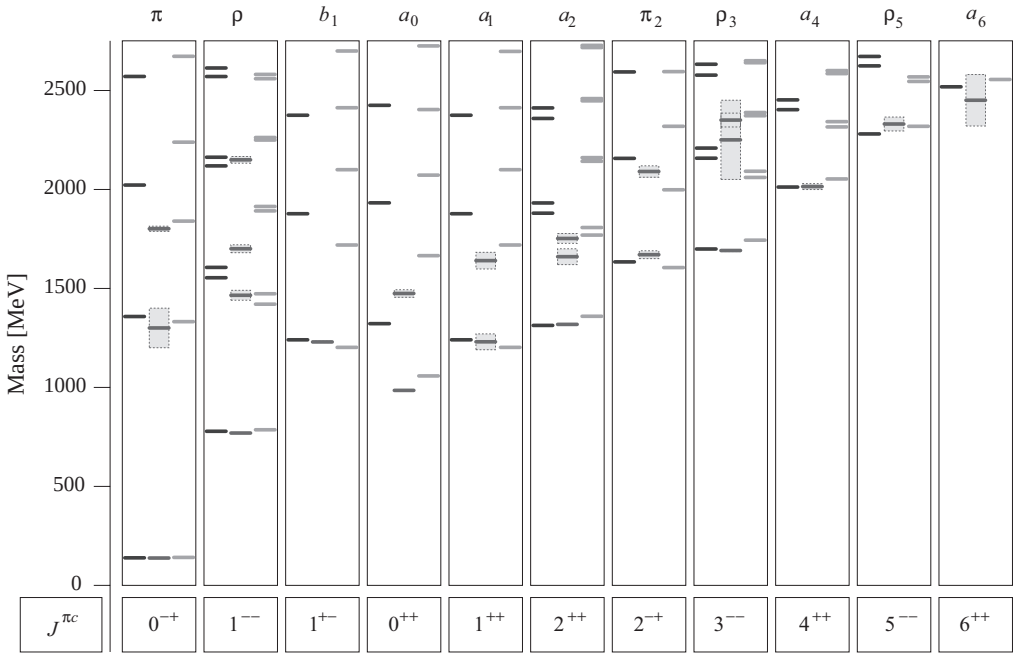

Fig. 1. The spectrum of the isovector mesons. The centric column shows the experimental data from [13]. Errors are indicated by shadowed boxes. The left and right columns show our results with model $\mathcal{A}$ and $\mathcal{B}$, respectively.

shown in figs. 2-4 and tables 2-4. We find good agreement for the heavy-light mesons in both models with small advantages in model $\mathcal{B}$ due to a larger spin-orbit splitting. Also the gross structure of the heavy-quarkonia spectra can be reproduced, but fine and hyperfine splittings come out too small. This is due to the missing of a substantial spin-orbit and spin-spin interaction, as provided, *e.g.*, by the one-gluon exchange potential. The radial excitations of the Υ, on the other hand, are excellently reproduced in model $\mathcal{B}$ up to the $5s$ state. Thus, we think that we have reached a good overall agreement with the experimental heavy masses and therefore have gained a good estimate for the heavy-meson amplitudes. To test these amplitudes further we investigate the semileptonic decays of heavy to light mesons. The relevant current matrix elements are calculated in lowest order after the prescription of Mandelstam [14]. In our formalism this leads in general to

$$\langle P'|J^\mu(q)|P\rangle = \int \frac{\mathrm{d}^4p}{(2\pi)^4} \mathrm{tr}\left[\bar{\Gamma}^{P'}\left(p-\frac{q}{2}\right) S_1^F\left(\frac{P}{2}+p-q\right) \times J^\mu S_1^F\left(\frac{P}{2}+p\right)\Gamma^P(p) S_2^F\left(-\frac{P}{2}+p\right)\right] \tag{5}$$

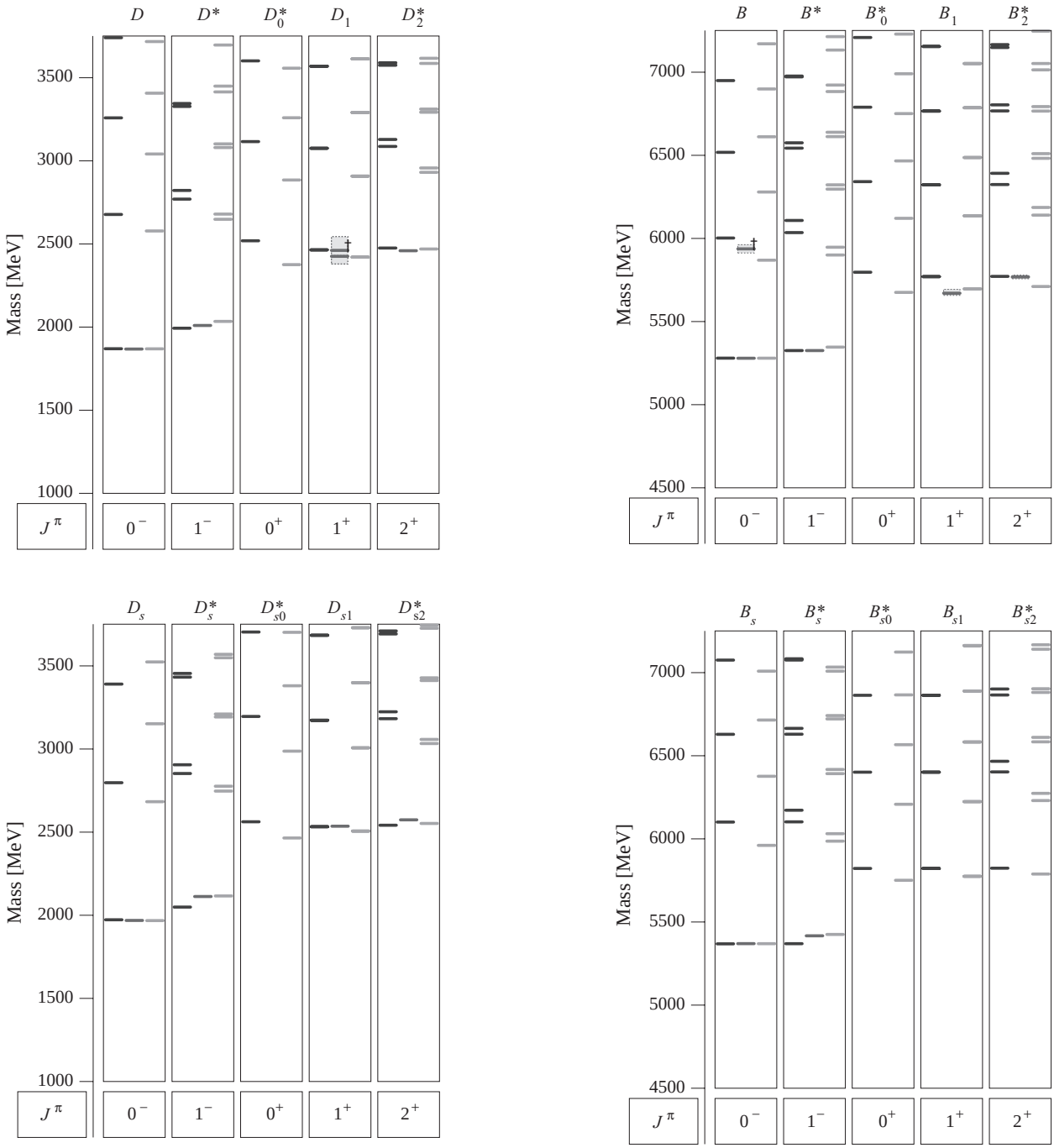

Fig. 2. The spectra of the charmed D and D_s mesons. The centric column shows the experimental data from [13]. Errors are indicated by shadowed boxes. The levels marked with † are taken from [15]. The upper and lower columns show our results with model $\mathcal{A}$ and $\mathcal{B}$, respectively. Note that the 1^+ states are twofold degenerated in our calculation corresponding to the total spin $S = 0$ and $S = 1$.

Fig. 3. The spectra of the bottom B and B_s mesons. The centric column shows the experimental data from [13]. Errors are indicated by shadowed boxes. The levels marked with † are taken from [1]. The upper and lower columns show our results with model $\mathcal{A}$ and $\mathcal{B}$, respectively. Note that the 1^+ states are twofold degenerated in our calculation corresponding to the total spin $S = 0$ and $S = 1$.

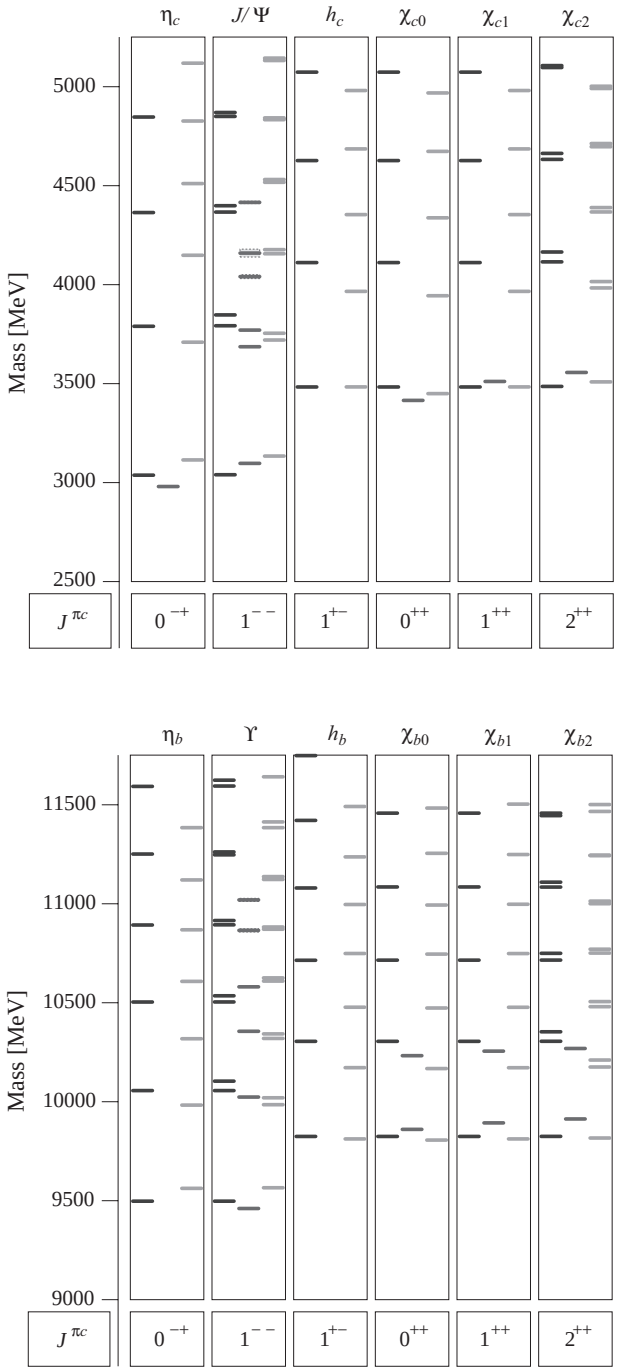

Fig. 4. The spectra of heavy quarkonia. The centric column shows the experimental data from [13]. Errors are indicated by shadowed boxes. The upper and lower columns show our results with model $\mathcal{A}$ and $\mathcal{B}$, respectively.

with the vertex function

$$\Gamma^P(p) := \left[S_1^F(\frac{P}{2}+p)\right]^{-1} \chi^P(p) \left[S_2^F(-\frac{P}{2}+p)\right]^{-1}. \quad (6)$$

In the instantaneous approximation the vertex function in the rest frame of the meson can be easily reconstructed from the Salpeter amplitude according to

$$\Gamma^P(p)|_{P=(M,\mathbf{0})} = -i\int\frac{\mathrm{d}^3p'}{(2\pi)^3}V(\mathbf{p},\mathbf{p}')\Phi(\mathbf{p}'). \quad (7)$$

Thus, the full 4-dimensional vertex function is known in the rest frame. Formal covariance of our model then allows to calculate the vertex function of any meson on its mass shell, which is essential for the calculation of meson decays.

3 Semileptonic decays

The effective Lagrangian for the semileptonic decays, *e.g.* $b \to c$ transitions, after integrating out the W-boson, has the usual $V-A$ current-current form

$$\mathcal{L}_{cb}^{\mathrm{eff}} = -\frac{G_F}{\sqrt{2}}\, V_{cb}\, \bar{c}\gamma^\mu(1-\gamma^5)b\; \bar{\ell}\gamma_\mu(1-\gamma^5)\nu \quad (8)$$

with the Cabibbo-Kobayashi-Maskawa (CKM) matrix element V_{cb}. Whereas the matrix elements of the leptonic current can be calculated exactly, those of the vector (V^μ) and axial vector (A^μ) hadronic currents are parametrized by form factors, reflecting the hadronic structure. A common parametrization is [16],

for a $0^- \to 0^-$ transition, *e.g.*, $B \to D\ell\bar{\nu}_\ell$:

$$\langle D|V^\mu|B\rangle = f_+(q^2)(P_B^\mu + P_D^\mu) + f_-(q^2)(P_B^\mu - P_D^\mu) \quad (9)$$

and a $0^- \to 1^-$ transition, *e.g.*, $B \to D^*\ell\bar{\nu}_\ell$:

$$\langle D^*|V^\mu|B\rangle = \frac{2i}{m_B+m_{D^*}}\varepsilon^\mu{}_{\nu\rho\sigma}\varepsilon^{*\nu}P_B^\rho P_{D^*}^\sigma V(q^2) \quad (10)$$

and

$$\begin{aligned}\langle D^*|A^\mu|B\rangle &= 2m_{D^*}\frac{\varepsilon^*\cdot q}{q^2}q^\mu A_0(q^2)\\ &-\frac{\varepsilon^*\cdot q}{m_B+m_{D^*}}\left(P_B^\mu + P_{D^*}^\mu - \frac{m_B^2-m_{D^*}^2}{q^2}q^\mu\right)A_2(q^2)\\ &+(m_B+m_{D^*})\left(\varepsilon^{*\mu}-\frac{\varepsilon^*\cdot q}{q^2}q^\mu\right)A_1(q^2), \end{aligned} \quad (11)$$

where $q = P_B - P_{D^{(*)}}$ is the momentum transfer and ε the polarization vector of the vector meson. In the limit of vanishing lepton mass only 4 of these 6 form factors contribute to the decay rates, namely f_+, V, A_1 and A_2, since terms proportional to q^μ can be neglected. Then, the differential decay rates, expressed in terms of these form factors, are

$$\frac{\mathrm{d}\Gamma^{0^-\to 0^-}}{\mathrm{d}q^2} = |V_{cb}|^2\frac{G_F^2}{24\pi^3}P_D^3|f_+|^2, \quad (12)$$

$$\frac{\mathrm{d}\Gamma^{0^-\to 1^-}}{\mathrm{d}q^2} = |V_{cb}|^2\frac{G_F^2}{(2\pi)^3}\frac{q^2P_{D^*}}{12m_B^2}\left(|H_+|^2+|H_-|^2+|H_0|^2\right), \quad (13)$$

Table 2. Masses of the charmed D and D_s mesons in MeV, calculated in model $\mathcal{A}$ and $\mathcal{B}$; n denotes the radial excitation. Note that the 1^+ states are twofold degenerated corresponding to the total spin $S = 0$ and $S = 1$.

Meson (J^π)	n	Model $\mathcal{A}$	Model $\mathcal{B}$	Meson (J^π)	n	Model $\mathcal{A}$	Model $\mathcal{B}$
$D(0^-)$	0	1869	1869	$D_s(0^-)$	0	1969	1969
	1	2677	2578		1	2794	2683
	2	3258	3041		2	3388	3152
$D^*(1^-)$	0	1993	2034	$D_s^*(1^-)$	0	2049	2116
	1	2769	2648		1	2852	2746
	2	2822	2679		2	2905	2776
	3	3327	3079		3	3432	3192
	4	3344	3101		4	3454	3210
$D_0^*(0^+)$	0	2519	2375	$D_{s0}^*(0^+)$	0	2563	2464
	1	3115	2884		1	3196	2986
$D_1(1^+)$	0	2464	2420	$D_{s1}(1^+)$	0	2532	2506
	1	2464	2420		1	2532	2506
	2	3075	2908		2	3172	3007
	3	3075	2908		3	3172	3007
$D_2^*(2^+)$	0	2475	2469	$D_{s2}^*(2^+)$	0	2541	2552
	1	3086	2930		1	3182	3032
	2	3128	2957		2	3223	3057

Table 3. Masses of the bottom B and B_s mesons in MeV, calculated in model $\mathcal{A}$ and $\mathcal{B}$; n denotes the radial excitation. Note that the 1^+ states are twofold degenerated corresponding to the total spin $S = 0$ and $S = 1$.

Meson (J^π)	n	Model $\mathcal{A}$	Model $\mathcal{B}$	Meson (J^π)	n	Model $\mathcal{A}$	Model $\mathcal{B}$
$B(0^-)$	0	5279	5279	$B_s(0^-)$	0	5368	5369
	1	6002	5869		1	6101	5960
	2	6517	6279		2	6628	6376
$B^*(1^-)$	0	5325	5346	$B_s^*(1^-)$	0	5369	5425
	1	6035	5900		1	6102	5986
	2	6108	5947		2	6172	6031
	3	6543	6296		3	6629	6392
	4	6575	6322		4	6664	6417
$B_0^*(0^+)$	0	5796	5675	$B_{s0}^*(0^+)$	0	5822	5750
	1	6341	6120		1	6401	6208
$B_1(1^+)$	0	5770	5696	$B_{s1}(1^+)$	0	5822	5774
	1	5770	5696		1	5822	5774
	2	6322	6136		2	6401	6224
	3	6322	6136		3	6401	6224
$B_2^*(2^+)$	0	5771	5711	$B_{s2}^*(2^+)$	0	5823	5788
	1	6324	6140		1	6402	6230
	2	6391	6186		2	6466	6273

Table 4. Masses of the heavy quarkonia in MeV, calculated in model $\mathcal{A}$ and $\mathcal{B}$; n denotes the radial excitation.

Meson ($J^{\pi c}$)	n	Model $\mathcal{A}$	Model $\mathcal{B}$	Meson ($J^{\pi c}$)	n	Model $\mathcal{A}$	Model $\mathcal{B}$
$\eta_c(0^{-+})$	0	3037	3114	$\eta_b(0^{-+})$	0	9497	9562
	1	3789	3708		1	10055	9983
	2	4363	4147		2	10503	10318
$J/\Psi(1^{--})$	0	3039	3133	$\Upsilon(1^{--})$	0	9497	9565
	1	3792	3719		1	10055	9985
	2	3846	3754		2	10103	10020
	3	4366	4155		3	10503	10319
	4	4398	4176		4	10534	10342
					5	10892	10609
					6	10914	10625
					7	11250	10871
					8	11261	10882
$h_c(1^{+-})$	0	3482	3483	$h_b(1^{+-})$	0	9824	9811
	1	4110	3965		1	10304	10171
$\chi_{c0}(0^{++})$	0	3482	3449	$\chi_{b0}(0^{++})$	0	9824	9805
	1	4110	3943		1	10304	10166
$\chi_{c1}(1^{++})$	0	3482	3483	$\chi_{b1}(1^{++})$	0	9824	9811
	1	4110	3965		1	10304	10171
$\chi_{c2}(2^{++})$	0	3485	3508	$\chi_{b2}(2^{++})$	0	9824	9816
	1	4114	3983		1	10304	10175
	2	4164	4015		2	10352	10210

where we have introduced the helicity amplitudes

$$H_\pm(q^2) := (m_B+m_{D^*})A_1(q^2) \mp \frac{2m_B P_{D^*}}{m_B+m_{D^*}} V(q^2), \quad (14)$$

$$H_0(q^2) := \frac{m_B^2 - m_{D^*}^2 - q^2}{2m_{D^*}\sqrt{q^2}}(m_B + m_{D^*})A_1(q^2) - \frac{2m_B^2 P_{D^*}^2}{m_{D^*}(m_B + m_{D^*})\sqrt{q^2}} A_2(q^2). \quad (15)$$

With regard to the processes $B \to D^{(*)}\ell\bar{\nu}$, that is the transition between heavy flavours, we want to summarize the predictions of heavy-flavour symmetry. For these transitions, the Heavy-Quark Effective Theorie (HQET) provides the appropriate framework. It is based on a systematic expansion in the inverse quark mass and has been worked out by Isgur and Wise [17,18]. In the limit $m_Q \to \infty$ the theory will become independent of the heavy degrees of freedom. For the spectra of heavy hadrons this will lead to degenerated doublets, corresponding to the two possible alignments of the heavy-quark spin. Recent experimental results show evidence for this degeneracy in the spectrum of the D-mesons [15]. For semileptonic decays HQET predicts a connection between the form factors of $0^- \to 0^-$ and $0^- \to 1^-$ transitions. In particular, in the infinite quark mass limit, the transition matrix elements can be expressed by a single function only, the Isgur-Wise function ξ, which is normalized to unity at maximum recoil.

In this heavy-quark limit it is more natural to express the decay amplitudes in terms of velocities rather than momenta and to introduce the dimensionless variable $\omega := v_B v_{D^{(*)}} = \left(m_B^2 + m_{D^{(*)}}^2 - q^2\right) / \left(2m_B m_{D^{(*)}}\right)$ instead of the momentum transfer q^2. Therefore, a new set of form factors is used [16], defined by

$$0^- \to 0^- \ : \quad \frac{\langle D|V^\mu|B\rangle}{\sqrt{m_B m_D}} = h_+(\omega)(v_B^\mu + v_D^\mu) + h_-(\omega)(v_B^\mu - v_D^\mu), \quad (16)$$

$$0^- \to 1^- \ : \quad \frac{\langle D^*|V^\mu|B\rangle}{\sqrt{m_B m_{D^*}}} = i\varepsilon^\mu{}_{\nu\rho\sigma}\varepsilon^{*\nu} v_B^\rho v_{D^*}^\sigma \, h_V(\omega),$$

$$\frac{\langle D^*|A^\mu|B\rangle}{\sqrt{m_B m_{D^*}}} = \varepsilon^{*\mu}(\omega+1)\, h_{A_1}(\omega) - v_B^\mu \varepsilon^* \cdot v_{D^*}\, h_{A_2}(\omega) - v_{D^*}^\mu \varepsilon^* \cdot v_B\, h_{A_3}(\omega), \quad (17)$$

with

$$m_Q \to \infty \quad : \quad h_V = h_{A_1} = h_{A_3} = h_+ = \xi \qquad h_{A_2} = h_- = 0 \quad (18)$$

in the infinite quark mass limit. The differential decay rates are given in this framework most conveniently by

$$\frac{\mathrm{d}\Gamma^{0^-\to 0^-}}{\mathrm{d}\omega} = \frac{G_F^2}{48\pi^3} m_D^3 (m_B+m_D)^2 \times (\omega^2-1)^{3/2} |V_{cb}|^2 \mathcal{G}^2(\omega), \quad (19)$$

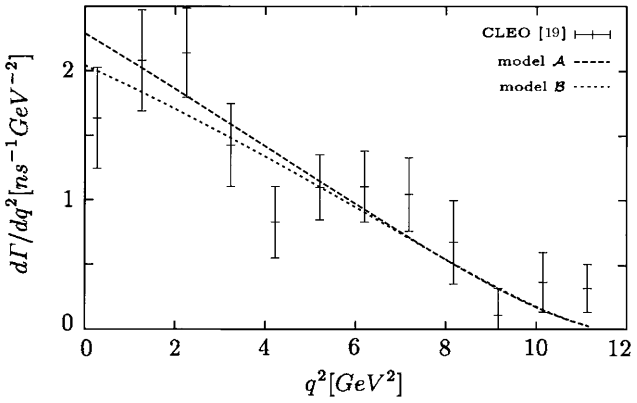

Fig. 5. The differential decay rate for $B \to D\ell\bar{\nu}$. The data are taken from [19]. The values of $|V_{cb}|$ corresponding to our calculations are $|V_{cb}| = 0.034$ and $|V_{cb}| = 0.035$ for model $\mathcal{A}$ and $\mathcal{B}$, respectively.

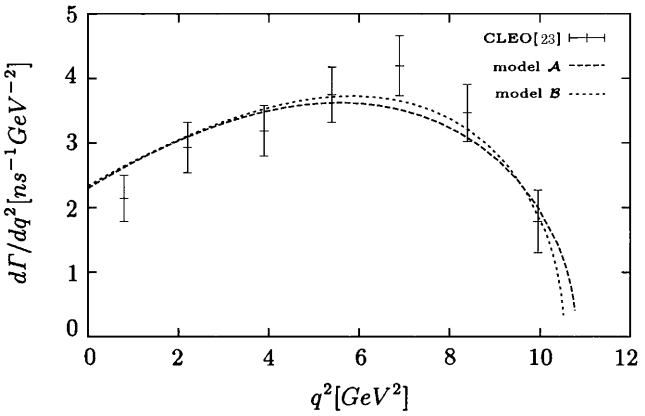

Fig. 6. The differential decay rate for $B \to D^*\ell\bar{\nu}$. The data are taken from [23]. The values of $|V_{cb}|$ corresponding to our calculations are $|V_{cb}| = 0.034$ and $|V_{cb}| = 0.035$ for model $\mathcal{A}$ and $\mathcal{B}$, respectively.

$$\frac{\mathrm{d}\Gamma^{0^-\to 1^-}}{\mathrm{d}\omega} = \frac{G_F^2}{48\pi^3} m_{D^*}^3 (m_B - m_{D^*})^2 \sqrt{\omega^2-1}(\omega+1)^2 \cdot \left[1 + \frac{4\omega}{\omega+1}\frac{1-2\omega r_* + r_*^2}{(1-r_*)^2}\right] |V_{cb}|^2 \mathcal{F}^2(\omega), \quad (20)$$

with $r_* = m_{D^*}/m_B$, where the two form factors $\mathcal{G}$ and $\mathcal{F}$ are functions of $h_\pm$ and h_V, h_{A_i}, respectively. This parametrization has the advantage that, for $m_Q \to \infty$, $\mathcal{F}$ and $\mathcal{G}$ become equal and coincide with the Isgur-Wise function ξ.

In the following sections our results for semileptonic B and charmed-meson decays are compared to the available experimental data and to the results of other models: the relativised constituent quark model of Isgur and Scora (ISGW2 [20]), the relativistic calculation of Wirbel, Stech and Bauer in the infinite-momentum frame (WSB [21]) and the relativistic dispersion relation approach of Melikhov and Stech (MS [22]). Since the experiments are not able to extract form factors from their measurements due to missing statistics, these are usually parametrized according to theoretical predictions. Therefore, we find it convenient to parameterize our results in the same way, allowing a comparison with experimental data. The accuracy of these parametrizations is always indicated.

3.1 Semileptonic decays of B-mesons

The decays $B \to D\ell\bar{\nu}_\ell$ and $B \to D^*\ell\bar{\nu}_\ell$ have been measured by Cleo [19,23,24] and, more recently, by Opal [25], Belle [26] and Delphi [27]. Figures 5 and 6 show our results for the differential decay rate compared to the Cleo data [19,23]. We find good overall agreement with the experimental data for both decays, using a CKM matrix element of $|V_{cb}| = 0.034 \pm 0.001$ and $|V_{cb}| = 0.035 \pm 0.001$ for model $\mathcal{A}$ and $\mathcal{B}$, respectively, which has been determined by a χ^2 fit. These values are somewhat smaller than the PDG average of $|V_{cb}| = 0.037$ to 0.043.

The resulting decay rates are

$$\begin{aligned} \text{model } \mathcal{A}: \quad & \Gamma(B \to D\ell\bar{\nu}_\ell) = 1.22 \cdot 10^{10}\,\mathrm{s}^{-1}, \\ & \Gamma(B \to D^*\ell\bar{\nu}_\ell) = 3.21 \cdot 10^{10}\,\mathrm{s}^{-1}, \\ \text{model } \mathcal{B}: \quad & \Gamma(B \to D\ell\bar{\nu}_\ell) = 1.14 \cdot 10^{10}\,\mathrm{s}^{-1}, \\ & \Gamma(B \to D^*\ell\bar{\nu}_\ell) = 3.24 \cdot 10^{10}\,\mathrm{s}^{-1}. \end{aligned}$$

The comparison with the current world average of the Particle Data Group [13],

$$\begin{aligned} \text{PDG}: \quad & \Gamma(B^+ \to \bar{D}^0\ell^+\nu_\ell) = 1.30 \pm 0.13 \cdot 10^{10}\,\mathrm{s}^{-1}, \\ & \Gamma(B^0 \to D^-\ell^+\nu_\ell) = 1.36 \pm 0.12 \cdot 10^{10}\,\mathrm{s}^{-1}, \\ & \Gamma(B^+ \to \bar{D}^{*0}\ell^+\nu_\ell) = 3.21 \pm 0.48 \cdot 10^{10}\,\mathrm{s}^{-1}, \\ & \Gamma(B^0 \to D^{*-}\ell^+\nu_\ell) = 2.97 \pm 0.17 \cdot 10^{10}\,\mathrm{s}^{-1}, \end{aligned}$$

as well as the recent data of Belle [26] and Delphi [27],

$$\begin{aligned} \text{Belle}: & \Gamma(\bar{B}^0 \to D^+\ell^-\bar{\nu}_\ell) = 1.38 \pm 0.08 \pm 0.25 \cdot 10^{10}\,\mathrm{s}^{-1}, \\ \text{Belle}: & \Gamma(\bar{B}^0 \to D^{*+}\ell^-\bar{\nu}_\ell) = 2.97 \pm 0.15 \pm 0.26 \cdot 10^{10}\,\mathrm{s}^{-1}, \\ \text{Delphi}: & \Gamma(\bar{B}^0 \to D^{*+}\ell^-\bar{\nu}_\ell) = 3.01 \pm 0.08^{+0.23}_{-0.20} \cdot 10^{10}\,\mathrm{s}^{-1}, \end{aligned}$$

shows satisfying agreement.

In table 5 our results for polarization ratios, defined by

$$\frac{\Gamma_L}{\Gamma_T} = \frac{\int \mathrm{d}q^2 q^2 P_{D^*} |H_0(q^2)|^2}{\int \mathrm{d}q^2 q^2 P_{D^*} \left(|H_+(q^2)|^2 + |H_-(q^2)|^2\right)}, \quad (21)$$

$$\frac{\Gamma_+}{\Gamma_-} = \frac{\int \mathrm{d}q^2 q^2 P_{D^*} |H_+(q^2)|^2}{\int \mathrm{d}q^2 q^2 P_{D^*} |H_-(q^2)|^2}, \quad (22)$$

are summarized. In these ($|V_{cb}|$ independent) quantities we find good agreement with the experimental values as well.

Table 5. $B \to D^{(*)}\ell\bar{\nu}$ decay observables and form factor parameters. We use $|V_{cb}| = 0.034(\mathcal{A})$, respectively, $|V_{cb}| = 0.035(\mathcal{B})$, as described in subsect. 3.1.

Parameter	Exp. [13]	Model $\mathcal{A}$	Model $\mathcal{B}$	ISGW2 [20]	WSB [21]	MS [22]
$\Gamma(B \to D)$ $\left(10^{13}\lvert V_{cb}\rvert^2\,\mathrm{s}^{-1}\right)$	—	1.05	0.93	1.19	0.808	0.86
$\Gamma(B \to D^*)$ $\left(10^{13}\lvert V_{cb}\rvert^2\,\mathrm{s}^{-1}\right)$	—	2.78	2.64	2.48	2.19	2.28
Γ_L/Γ_T	1.24 ± 0.16 [28]	1.14	1.20	1.04	—	1.11
Γ_+/Γ_-	—	0.23	0.27	—	—	—
R_1	$1.18 \pm 0.30 \pm 0.12$	1.18	1.10	1.27	$1.09^{(a)}$	—
R_2	$0.71 \pm 0.22 \pm 0.07$	0.94	0.87	1.02	$1.06^{(a)}$	—
$\rho^2_{A_1}$	$0.91 \pm 0.15 \pm 0.06$	0.75	1.02	—	—	—

$^{(a)}$ Taken from [16].

We also show the results for the form factor ratios

$$R_1 := \frac{h_V(\omega)}{h_{A_1}(\omega)} = \left(1 - \frac{q^2}{(m_B + m_{D^*})^2}\right) \frac{V(q^2)}{A_1(q^2)}, \quad (23)$$

$$R_2 := \frac{h_{A_3}(\omega) + \frac{m_{D^*}}{m_B} h_{A_2}(\omega)}{h_{A_1}(\omega)} = \left(1 - \frac{q^2}{(m_B + m_{D^*})^2}\right) \frac{A_2(q^2)}{A_1(q^2)}. \quad (24)$$

In the heavy-quark limit these ratios are predicted to be constant and equal to unity. In reality, due to corrections to this limit, R_1 and R_2 do depend on ω, but at the scale of the b-quark mass this dependency is expected to be very weak. Therefore these ratios are prefered in the analysis of $B \to D^*\ell\bar{\nu}$, where they are assumed to be constant, whereas h_{A_1} is approximated by a linear or quadratic function

$$h_{A_1}(\omega) \approx h_{A_1}(1)\left(1 - \rho^2_{A_1}(\omega - 1) + \lambda_{A_1}(\omega - 1)^2\right). \quad (25)$$

For our form factors the ω-dependency of $R_{1/2}$ is less than 2%, and the mean values are shown in table 5. The form factor h_{A_1} can be described by the parametrization (25) with an accuracy of 0.1% (0.3%) for model $\mathcal{A}(\mathcal{B})$, yielding

$$\begin{aligned} &\text{model } \mathcal{A}: \quad h_{A_1}(1) = 0.97, \quad \rho^2_{A_1} = 0.73, \quad \lambda_{A_1} = 0.27, \\ &\text{model } \mathcal{B}: \quad h_{A_1}(1) = 1.01, \quad \rho^2_{A_1} = 0.98, \quad \lambda_{A_1} = 0.48, \end{aligned}$$

which is in good agreement with the experimental data shown in table 5.

Two recent measurements of $B \to D^*\ell\bar{\nu}$ by the CLEO [24] and the OPAL [25] collaborations have been published, where a different parametrization of the form factor based on dispersion relations has been used. These analyses expand h_{A_1} in the variable $z(\omega) = (\sqrt{\omega+1} - \sqrt{2})/(\sqrt{\omega+1} + \sqrt{2})$ and use the parametrization [29]

$$h_{A_1}(\omega)/h_{A_1}(1) = 1 - 8\rho^2 z + (53\rho^2 - 15)z^2 - (231\rho^2 - 91)z^3$$

with the (inconsistent) results

$$\begin{aligned} &\text{OPAL [25]}: \rho^2 = 1.21 \pm 0.12 \pm 0.20, \\ &\text{CLEO [24]}: \rho^2 = 1.67 \pm 0.11 \pm 0.22. \end{aligned}$$

A similar fit to our form factor gives

$$\text{model } \mathcal{A}: \rho^2 = 0.83, \qquad \text{model } \mathcal{B}: \rho^2 = 1.06,$$

with an accuracy of 1% and 0.4% for model $\mathcal{A}$ and $\mathcal{B}$, respectively. Thus, our calculation is rather compatible with the OPAL result.

To connect our results with the description in the framework of HQET, we have calculated the form factors $\mathcal{F}$ and $\mathcal{G}$ (see eq. (20)) and their slopes at $\omega = 1$ by fitting a quadratic function analogous to (25). This is possible with an accuracy of 0.2% (0.3%) for model $\mathcal{A}(\mathcal{B})$ and gives the result

$$\begin{aligned} \text{model } \mathcal{A}: \quad &\mathcal{G}(1) = 1.01, \quad \rho^2_{\mathcal{G}} = 0.70, \quad \lambda_{\mathcal{G}} = 0.22, \\ &\mathcal{F}(1) = 0.97, \quad \rho^2_{\mathcal{F}} = 0.65, \quad \lambda_{\mathcal{F}} = 0.20, \\ \text{model } \mathcal{B}: \quad &\mathcal{G}(1) = 1.01, \quad \rho^2_{\mathcal{G}} = 0.85, \quad \lambda_{\mathcal{G}} = 0.31, \\ &\mathcal{F}(1) = 1.01, \quad \rho^2_{\mathcal{F}} = 0.91, \quad \lambda_{\mathcal{F}} = 0.56. \end{aligned}$$

These quantities $\mathcal{G}(1)$ and $\mathcal{F}(1)$ have been calculated in the HQET. Current values are [13]:

$$\mathcal{G}(1) = 1.00 \pm 0.07, \qquad \mathcal{F}(1) = 0.92 \pm 0.05.$$

Finally, we have performed the heavy-quark limit numerically in our model by scaling the quark masses with a large factor. We find that the form factors then indeed coincide or vanish (see eq. (18)). The resulting universal function $\tilde{\xi}$, which we identify as the Isgur-Wise function of our model, can be parametrized up to deviations of less than 0.2% and 0.5% for model $\mathcal{A}$ and $\mathcal{B}$ as

$$\tilde{\xi}(\omega) = \tilde{\xi}(1)(1 - \rho^2_{\tilde{\xi}}(\omega - 1) + \lambda_{\tilde{\xi}}(\omega - 1)^2),$$

where

$$\begin{aligned} &\text{model } \mathcal{A}: \quad \tilde{\xi}(1) = 1.00, \quad \rho^2_{\tilde{\xi}} = 0.78, \quad \lambda_{\tilde{\xi}} = 0.31, \\ &\text{model } \mathcal{B}: \quad \tilde{\xi}(1) = 1.00, \quad \rho^2_{\tilde{\xi}} = 1.06, \quad \lambda_{\tilde{\xi}} = 0.50. \end{aligned}$$

In particular, we find that $\tilde{\xi}$ is indeed normalised to $\tilde{\xi}(1) = 1$. The ω-dependence is of course model dependent.

Table 6. $D \to K^{(*)}\ell\bar{\nu}$ decay observables and form factor parameters. The experimental decay rates are averaged over isospin. We use $|V_{cs}| = 0.975$ [13].

Parameter	Exp. [13]	Model $\mathcal{A}$	Model $\mathcal{B}$	ISGW2 [20]	WSB [21]	MS [22]
$\Gamma(D \to K)$ $\left(10^{10}\,\mathrm{s}^{-1}\right)$	7.97 ± 0.36	7.51	7.26	10.0	8.26	9.7
$\Gamma(D \to K^*)$ $\left(10^{10}\,\mathrm{s}^{-1}\right)$	4.55 ± 0.34	7.64	10.08	5.4	9.53	6.0
Γ_L/Γ_T	1.14 ± 0.08	1.29	1.48	0.94	0.91	1.28
Γ_+/Γ_-	0.21 ± 0.04	0.23	0.34	—	—	—
$A_1(0)$	0.56 ± 0.04 [16]	0.69	0.81	—	0.88	0.66
r_V	1.82 ± 0.09	1.54	1.18	$2.0^{(a)}$	1.44	1.56
r_2	0.78 ± 0.07	0.81	0.62	$1.3^{(a)}$	1.31	0.74

$^{(a)}$ Taken from [30].

Table 7. $D_s \to \eta/\eta'/\phi\ell\bar{\nu}$ decay observables and form factor parameters. The experimental decay rates are averaged over isospin. We use $|V_{cs}| = 0.975$ [13].

Parameter	Exp. [13]	Model $\mathcal{A}$	Model $\mathcal{B}$	ISGW2 [20]	WSB [21]	MS [22]
$\Gamma(D_s \to \eta)$ $\left(10^{10}\,\mathrm{s}^{-1}\right)$	5.24 ± 1.41	4.05	3.11	$3.5^{(a)}$	—	5.0
$\Gamma(D_s \to \eta')$ $\left(10^{10}\,\mathrm{s}^{-1}\right)$	1.80 ± 0.69	1.27	1.75	$3.0^{(a)}$	—	1.85
$\Gamma(D_s \to \phi)$ $\left(10^{10}\,\mathrm{s}^{-1}\right)$	4.03 ± 1.01	7.89	9.67	4.6	—	5.1
Γ_L/Γ_T	0.72 ± 0.18	1.20	1.42	0.96	—	—
Γ_+/Γ_-	—	0.20	0.33	—	—	—
$A_1(0)$	—	0.66	0.79	—	—	0.65
r_V	1.92 ± 0.32	1.77	1.30	$2.1^{(b)}$	—	1.71
r_2	1.60 ± 0.24	0.85	0.63	$1.3^{(b)}$	—	0.72

$^{(a)}$ A η-η' mixing angle of -20° is assumed. An angle of -10° would lead to 5.3 and 2.3.
$^{(b)}$ Taken from [31].

3.2 Semileptonic decays of charmed mesons

The semileptonic decays of charmed mesons, induced by the quark level process $c \to s$, have been measured for the $D \to K^{(*)}$ as well as for the $D_s \to \eta/\eta'/\phi$ transitions. The results, averaged over isospin, are shown in tables 6 and 7. For the D-meson decay $D \to K\ell\bar{\nu}$ the comparison with our calculation shows reasonable agreement for both models. The decay to the K^* final state however is overestimated by about a factor of 2. The polarization observables on the other hand are comparable with the experimental result, whereby model $\mathcal{A}$ gives better agreement than model $\mathcal{B}$. This is a well-known problem of constituent quark models. Our results are rather comparable with those of Wirbel *et al.* (WSB [21]). With respect to the ISGW2 [20] predictions it is interesting to note that, whereas the inclusion of relativistic corrections was one of the main ingredients in their model to decrease the $D \to K^*$ decay rate, this problem still exists in our full relativistic calculation.

Apart from the decay rates and the polarization observables, the form factor ratios at zero-momentum transfer, defined by

$$r_V := \frac{V(0)}{A_1(0)}, \qquad r_2 := \frac{A_2(0)}{A_1(0)}, \tag{26}$$

are considered. To extract these ratios from experiment the form factors are usually parametrized by a simple pole ansatz with a pole mass of 2.1 GeV for the vector form factor and 2.5 GeV for the axial form factors. We have performed such a fit to our calculations, which works up to deviations of about 6% for the form factors and of 4% for their ratios, and have extracted the form factor ratios for D-meson decays from these parametrizations. The results in table 6 show that the axial form factors are generally overrated, while our vector form factor parameters agree with the values extracted from experiment. Thus the failure in the $D \to K^{(*)}$ decay rate can be traced back to this overestimation of the axial form factors.

In this connection it is interesting to estimate the effect of the full relativistic treatment. In figs. 7-9 the positive and negative energy radial amplitudes of the D, D^* and B mesons are plotted. It shows that at least for the D-meson the negative energy comonents are not small. If we neglect these components of the Salpeter amplitude when reconstructing the vertex function, we can see their impact on the current matrix elements: With this reduced vertex function the form factor ratios r_V and r_2 are calculated. Hereby, we concentrate on model $\mathcal{A}$, since, as has been discussed in [12], the positive and negative

Table 8. $D \to \pi/\rho\ell\bar{\nu}$ decay observables and form factor parameters. We use $|V_{cd}| = 0.222$ [13].

Parameter	Exp. [13]	Model $\mathcal{A}$	Model $\mathcal{B}$	ISGW2 [20]	WSB [21]	MS [22]
$\Gamma(D^+ \to \pi^0)$ $\left(10^9\,\mathrm{s}^{-1}\right)$	2.9 ± 1.4	1.03	0.99	2.4	3.6	4.8
$\Gamma(D^0 \to \pi^-)$ $\left(10^9\,\mathrm{s}^{-1}\right)$	9.0 ± 1.5	2.06	1.99	4.8	7.1	9.6
$\Gamma(D^+ \to \rho^0)$ $\left(10^9\,\mathrm{s}^{-1}\right)$	2.1 ± 0.8	2.25	3.36	1.2	3.4	2.1
Γ_L/Γ_T	—	1.30	1.55	0.67	0.91	1.16
Γ_+/Γ_-	—	0.15	0.26	—	—	—
$A_1(0)$	—	0.58	0.72	—	0.78	0.6
r_V	—	1.68	1.26	—	1.58	1.48
r_2	—	0.77	0.59	—	1.18	0.82

Table 9. $D \to \eta/\eta'/\omega\ell\bar{\nu}$ decay observables and form factor parameters. We use $|V_{cd}| = 0.222$ [13].

Parameter	Exp. [13]	Model $\mathcal{A}$	Model $\mathcal{B}$	ISGW2 [20]	WSB [21]	MS [22]
$\Gamma(D \to \eta)$ $\left(10^9\,\mathrm{s}^{-1}\right)$	—	0.79	0.95	1.5 [(a)]	—	—
$\Gamma(D \to \eta')$ $\left(10^9\,\mathrm{s}^{-1}\right)$	—	0.14	0.16	0.3 [(a)]	—	—
$\Gamma(D \to \omega)$ $\left(10^9\,\mathrm{s}^{-1}\right)$	—	2.23	3.35	1.2	—	—
Γ_L/Γ_T	—	1.31	1.55	0.68	—	—
Γ_+/Γ_-	—	0.15	0.26	—	—	—
$A_1(0)$	—	0.41	0.51	—	—	—
r_V	—	1.68	1.27	—	—	—
r_2	—	0.77	0.59	—	—	—

[(a)] A η-η' mixing angle of $-20°$ is assumed. An angle of $-10°$ would lead to 1.1 and 0.4.

Table 10. $D_s \to K/K^*\ell\bar{\nu}$ decay observables and form factor parameters. We use $|V_{cd}| = 0.222$ [13].

Parameter	Exp. [13]	Model $\mathcal{A}$	Model $\mathcal{B}$	ISGW2 [20]	WSB [21]	MS [22]
$\Gamma(D_s \to K)$ $\left(10^9\,\mathrm{s}^{-1}\right)$	—	3.42	3.15	4.4	—	6.4
$\Gamma(D_s \to K^*)$ $\left(10^9\,\mathrm{s}^{-1}\right)$	—	2.71	4.54	2.2	—	3.9
Γ_L/Γ_T	—	1.24	1.51	0.76	—	1.21
Γ_+/Γ_-	—	0.14	0.29	—	—	—
$A_1(0)$	—	0.43	0.58	—	—	0.57
r_V	—	1.86	1.26	—	—	1.83
r_2	—	0.76	0.56	—	—	0.74

energy components of the Salpeter amplitude decouple in the non-relativistic reduction of the Salpeter equation. We then find that these ratios slightly rise: r_V changes from 1.48 to 1.55, r_2 goes from 0.78 up to 0.84 [2], while the q^2-dependence is hardly changed. Thus, the modification of a form factors by the full relativistic treatment seems to be more complex than the intuitive correction anticipated in [20].

The results on the semileptonic decays $D_s \to \eta$ and $D_s \to \eta'$ are shown in table 7. Here, it has to be stressed that the flavour mixing of η and η' had already been fixed by the mass fit. No additional mixing parameter is necessary. Although the differences between the results of our two models are rather large, the experimental data do not allow to prefer one of our parameter sets.

Our results on $D_s \to \phi$ show the same behaviour as those on $D \to K^*$: While the decay rate is overestimated by a factor of 2, the polarization observable is in good agreement with the experimental data and the form factor ratio r_V tends to be too small. Concerning the ratio of axial form factors it is interesting to note that the experimental value of r_2 is 4 standard deviations higher than the corresponding value for $D \to K^*$, which is in contradiction to an (approximate) flavour $SU(3)$ symmetry. This result, if it should be confirmed, is clearly a challenge for any theoretical description.

Finally, to conclude the discussion of charmed-meson decays, we report our results on the Cabibbo-suppressed

[2] These are the calulated values, not by results of the pole ansatz parametrization in table 6.

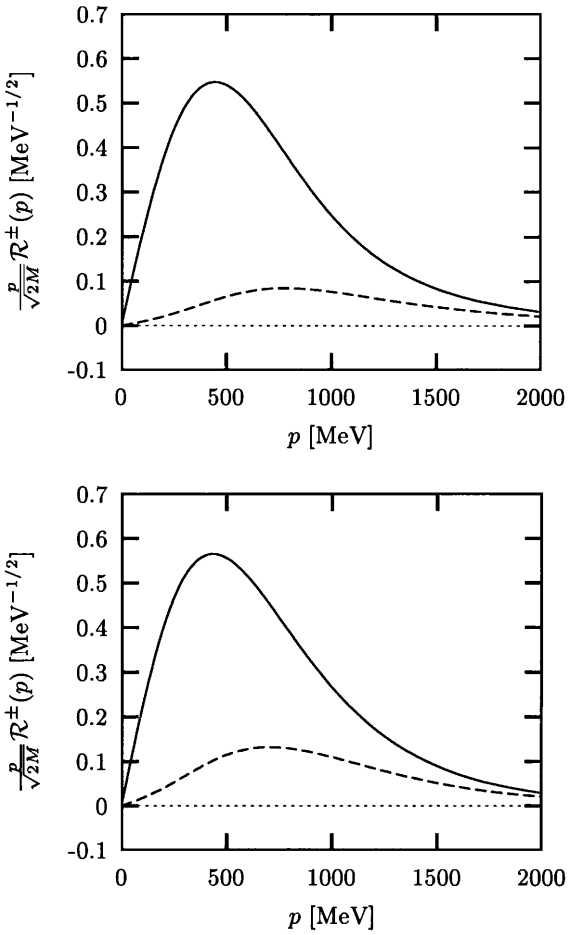

Fig. 7. Radial amplitudes $\mathcal{R}^{+}_{00}(p)$ (solid) and $\mathcal{R}^{-}_{00}(p)$ (dashed) of the D-meson Salpeter amplitude in model $\mathcal{A}$ (top) and $\mathcal{B}$ (bottom).

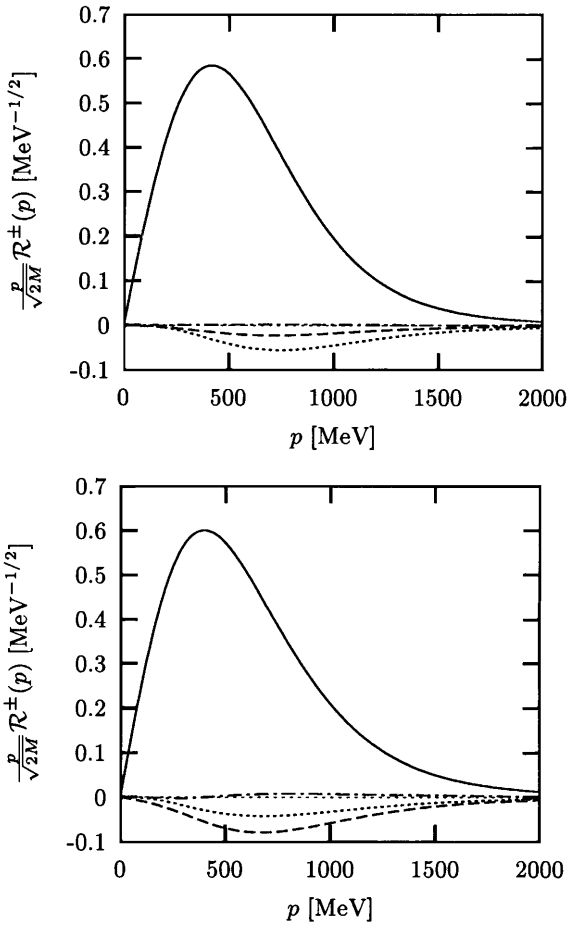

Fig. 8. Radial amplitudes $\mathcal{R}^{+}_{01}(p)$ (s-wave, solid), $\mathcal{R}^{+}_{21}(p)$ (d-wave, dash-dotted), $\mathcal{R}^{-}_{01}(p)$ (s-wave, dashed) and $\mathcal{R}^{-}_{21}(p)$ (d-wave, dotted) of the D^*-meson Salpeter amplitude in model $\mathcal{A}$ (top) and $\mathcal{B}$ (bottom).

process $c \to d$ in tables 8-10. The form factors again have been parametrized by a pole ansatz with pole masses of 2.0 GeV and 2.4 GeV for the vector and axial form factors respectively, which works up to deviations of 8% for $A_1(0)$ and 5% for the ratios. The current experimental situation, however, allows no evaluation of our description of these decays.

Thus, in summary, we find excellent agreement in the description of heavy-to-heavy transitions $B \to D^{(*)}$ over the whole kinematic regime. We find also consistency with the description of these processes in the framework of the HQET. The results on heavy-to-light transitions are mostly in agreement with the experimental data, but the common problem of quark models to overestimate the axial form factors is also present here.

4 Non-leptonic weak decays

To extract further information from our meson amplitudes we finally investigate non-leptonic decays. On tree level, non-leptonic decays are mediated by a single W-boson emission. Hard and soft gluonic effects however might play a significant role in these processes. These corrections have been calculated with great effort in the last years in order to extract model-independent Cabibbo-Kobayashi-Maskawa matrix elements or signatures for CP violation in B decays from experimental data. Thereby, the hard- and soft-gluon contributions are separated by a Wilson operator product expansion, which results in the effective Lagrangian, *e.g.*, for $B \to D\pi$ transitions,

$$\begin{aligned}\mathcal{L}^{\text{eff}}_{B\to D\pi} = -\frac{G_F}{\sqrt{2}}\, V_{cb}V^*_{du}\, \Big(&\frac{1}{2}a_1(\mu)(\bar{c}b)^{\mu}_{V-A}(\bar{d}u)_{\mu V-A}\\ &+\frac{1}{2}a_2(\mu)(\bar{d}b)^{\mu}_{V-A}(\bar{c}u)_{\mu V-A}\\ &+\frac{1}{2}C_1(\mu)(\bar{d}\lambda^A b)^{\mu}_{V-A}(\bar{c}\lambda^A u)_{\mu V-A}\\ &+\frac{1}{2}C_2(\mu)(\bar{c}\lambda^A b)^{\mu}_{V-A}(\bar{d}\lambda^A u)_{\mu V-A}\Big), \qquad (27)\end{aligned}$$

with $(\bar{c}\lambda^A b)^{\mu}_{V-A} := \bar{c}\gamma^{\mu}(1-\gamma^5)\lambda^A b$ etc., $a_1 := C_1 + \frac{1}{3}C_2$ and $a_2 := C_2 + \frac{1}{3}C_1$, where $C_{1/2}$ are the (scale dependent) Wilson coefficients, and λ^A the $SU(3)$ color Gell-Mann

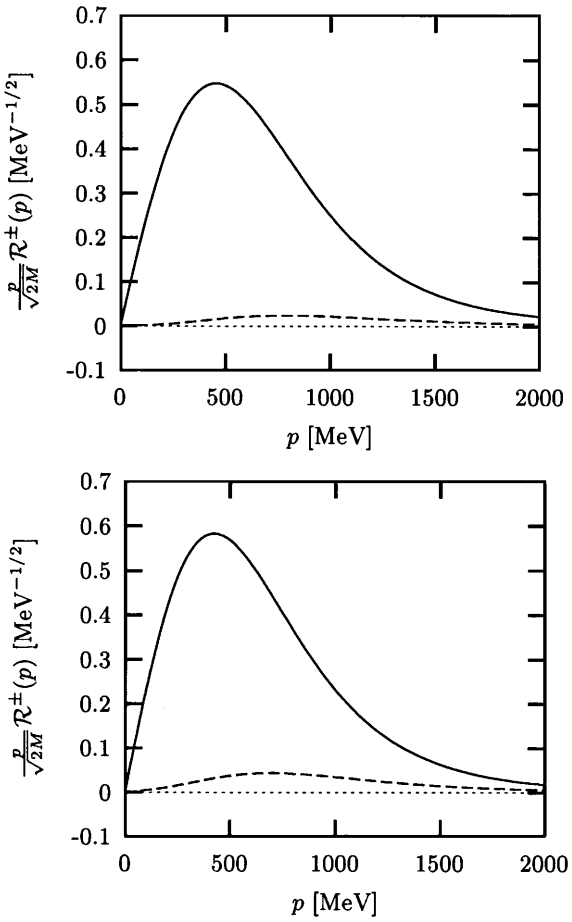

Fig. 9. Radial amplitudes $\mathcal{R}^{+}_{00}(p)$ (solid) and $\mathcal{R}^{-}_{00}(p)$ (dashed) of the B-meson Salpeter amplitude in model $\mathcal{A}$ (top) and $\mathcal{B}$ (bottom).

Table 11. Decay constants of pseudoscalar and pseudovector mesons in MeV.

Meson	Exp. [13]	Model $\mathcal{A}$	Model $\mathcal{B}$
π	$130.7 \pm 0.1 \pm 0.36$	212	219
K	$159.8 \pm 1.4 \pm 0.44$	248	238
D	$300\,^{+180+80}_{-150-40}$	293	263
D_s	$280 \pm 19 \pm 28 \pm 34$	315	284
ρ	216 ± 5 [32]	470	717
ω	195 ± 3 [32]	472	726
ϕ	237 ± 4 [32]	475	685
K^*	214 ± 7 [32]	467	695
D^*	—	339	409
D^*_s	—	378	445

matrices. Here we found it convenient to use an expression symmetric under Fierz transformation. The second line obviously does not contribute for color singlet states.

This Lagrangian gives rise to W emission diagrams. Contributions by weak annihilation and internal W exchange, which are suppressed by powers of $\Lambda_{\rm QCD}/m_b$, are neglected.

Table 12. Non-leptonic B-decay rates Γ (ns^{-1}). We use $|V_{cs}| = 0.975$, $|V_{ud}| = 0.975$, $|V_{us}| = 0.223$ [13] and $|V_{cb}| = 0.034$ ($\mathcal{A}$), respectively, $|V_{cb}| = 0.035$ ($\mathcal{B}$), as described in subsect. 3.1. The results of [32] have been adapted to the decay constants used in our calculation.

Decay mode	Exp. [13]	Model $\mathcal{A}$	Model $\mathcal{B}$	NRSX [32]
$B^0 \to D^- \pi^+$	1.94 ± 0.26	2.21	1.97	1.94
$B^0 \to D^- \rho^+$	5.10 ± 0.90	5.68	6.13	4.84
$B^0 \to D^{*-} \pi^+$	1.78 ± 0.14	2.22	1.88	1.87
$B^0 \to D^{*-} \rho^+$	4.4 ± 2.2	6.57	6.67	5.48
$B^0 \to D^- K^+$	—	0.17	0.15	0.15
$B^0 \to D^- K^{*+}$	—	0.31	0.30	0.26
$B^0 \to D^{*-} K^+$	—	0.16	0.14	0.14
$B^0 \to D^{*-} K^{*+}$	—	0.36	0.34	0.32
$B^0 \to D^- D^+$	—	0.53	0.49	0.23
$B^0 \to D^- D^{*+}$	—	0.37	0.34	0.23
$B^0 \to D^{*-} D^+$	—	0.39	0.41	0.17
$B^0 \to D^{*-} D^{*+}$	$0.40\,^{+0.26}_{-0.20}$	0.86	0.89	0.54
$B^+ \to \overline{D}^0 D^+_s$	7.9 ± 2.4	8.73	8.27	6.61
$B^0 \to D^- D^+_s$	5.2 ± 1.9	8.73	8.27	6.61
$B^+ \to \overline{D}^0 D^{*+}_s$	5.4 ± 2.4	6.05	5.49	6.15
$B^0 \to D^- D^{*+}_s$	6.5 ± 3.2	6.05	5.49	6.15
$B^+ \to \overline{D}^{*0} D^+_s$	7.3 ± 3.0	6.14	6.47	4.49
$B^0 \to D^{*-} D^+_s$	6.2 ± 2.2	6.14	6.47	4.49
$B^+ \to \overline{D}^{*0} D^{*+}_s$	16.3 ± 6.0	14.68	15.24	15.8
$B^0 \to D^{*-} D^{*+}_s$	12.9 ± 4.5	14.68	15.24	15.8

Thus, the matrix element of a product of currents has to be evaluated. This is usually done using the "factorization approximation", where one assumes that the amplitude is dominated by its factorizable part. Then it is given by the product of two current matrix elements, *e.g.*, for the transition $B^+ \to \overline{D}^0 \pi^+$:

$$A(B^+ \to \overline{D}^0 \pi^+) = \frac{G_F}{\sqrt{2}} V_{cb} V^*_{du} \Big\{ a_1 \langle \pi^+ | h_{\mu\, du} | 0 \rangle \langle \overline{D}^0 | h^{\mu}_{cb} | B^+ \rangle + a_2 \langle \overline{D}^0 | h_{\mu\, dc} | 0 \rangle \langle \pi^+ | h^{\mu}_{ub} | B^+ \rangle \Big\}. \quad (28)$$

In this way the decay amplitude can be expressed by the decay constant and a form factor of the semileptonic decay at the relevant q^2, *e.g.*,

$$\langle \pi^+ | J^\mu | 0 \rangle \langle \overline{D}^0 | J'_\mu | B^+ \rangle = \left(m_B^2 - m_D^2 \right) f_\pi F_0(m_\pi^2), \quad (29)$$

$$\langle \pi^+ | J^\mu | 0 \rangle \langle \overline{D^*}^0 | J'_\mu | B^+ \rangle = 2\varepsilon^* \cdot p_B m_{D^*} f_\pi A_0(m_\pi^2), \quad (30)$$

with the decay constants $\langle 0 | J^\mu | 0^- \rangle = i f P^\mu$, $\langle 0 | J^\mu | 1^- \rangle = m F \varepsilon^\mu$. It should be noted that the relevant form factors are F_0 and A_0, which are unimportant for semileptonic decays due to the smallness of the lepton mass. Hence nonleptonic decays offer a possibility to access the remaining semileptonic form factors, at least within the framework

Table 13. Ratios of non-leptonic B-meson decay rates.

Decay ratio	Exp. [13]	Model $\mathcal{A}$	Model $\mathcal{B}$	NRSX [32]
$\frac{\Gamma(B^0 \to D^- \pi^+)}{\Gamma(B^0 \to D^{*-} \pi^+)}$	1.09 ± 0.17	1.00	1.05	1.04
$\frac{\Gamma(B^0 \to D^- \rho^+)}{\Gamma(B^0 \to D^{*-} \rho^+)}$	1.16 ± 0.62	0.87	0.92	0.88
$\frac{\Gamma(B^0 \to D^- D_s^+)}{\Gamma(B^0 \to D^{*-} D_s^+)}$	0.83 ± 0.43	1.42	1.28	1.47
$\frac{\Gamma(B^+ \to \overline{D}^0 D_s^+)}{\Gamma(B^+ \to \overline{D}^{*0} D_s^+)}$	1.08 ± 0.56			
$\frac{\Gamma(B^0 \to D^- D_s^{*+})}{\Gamma(B^0 \to D^{*-} D_s^{*+})}$	0.50 ± 0.31	0.41	0.36	0.39
$\frac{\Gamma(B^+ \to \overline{D}^0 D_s^{*+})}{\Gamma(B^+ \to \overline{D}^{*0} D_s^{*+})}$	0.33 ± 0.19			

of the factorization approximation. The factorization assumption has been proven recently at two-loop order [33] for a special class of decays.

In this approach, however, the resulting amplitudes are scale dependent due to the μ-dependence of the Wilson coefficients, which is not canceled by the scale-independent matrix elements. To deal with this difficulty the coefficients a_1 and a_2 are often treated as effective and free parameters, corresponding to some factorization scale, to be extracted from the data. But since we are interested in an estimate of the quality of our form factors, we find it sufficient to neglect all strong gluonic effects, which results in $C_1 = 1, C_2 = 0 \equiv a_1 = 1, a_2 = \frac{1}{3}$ and restrict our calculation to the decays of B-mesons via the emission of a W-meson, usually called type-I decays.

The weak-decay constants are shown in table 11. Since these are generally overestimated in our models, which might be related to the instantaneous approximation or the constituent quark masses, as discussed in [2], we have used the experimental values, which are extracted from leptonic decay or τ-decay and are summarized in table 11. For the vector mesons D^* and D_s^*, where no data are available yet, we use $F_{D^*_{(s)}} \approx f_{D_{(s)}}$, which is valid in the heavy-quark limit. Deviations from this limit are expected to be about 10–20% [32]. The relevant CKM-matrix elements are taken from [13] except for V_{cb} where we use the fit results from subsect. 3.1.

Our results for non-leptonic B-decays are shown in table 12, compared with the experimental data from [13] as well as the calculation of Neubert *et al.* [32]. We find good agreement with the data available so far for both our models; and for those decays, which are not measured yet, our results are comparable with [32].

In order to stress the influence of our form factors, we show the ratios of decay rates (in which the decay constants as well as the coefficient a_1 cancel) in table 13. We also find good agreement with the experimental data, however the errors are quite large.

5 Summary

In this paper we have calculated the masses and the exclusive semileptonic and non-leptonic decays of heavy mesons in a constituent quark model based on the Bethe-Salpeter equation in instantaneous approximation. Apart from a linear confinement potential with two different phenomenological Dirac structures, a flavour-dependent residual interaction motivated by instanton effects is adopted, which has been naively generalized to heavy flavours. Thus, extending a very good description of light mesons, which has recently been updated in [2], we also find good overall agreement with the data on heavy-meson masses.

The resulting meson amplitudes are used to calculate semileptonic decay rates. We find excellent agreement in the description of heavy-to-heavy transitions $B \to D^{(*)}$ over the whole kinematic regime. Our results are also consistent with the description of these processes in the framework of the HQET. The results on heavy-to-light transitions are mostly in agreement with the experimental data, but the common problem of quark models to overestimate the axial form factors is also found here.

Finally, non-leptonic decays have then been calculated in the approximation of factorizing matrix elements. In spite of this simple picture, we find good agreement with the experimental results on B-meson decays.

Financial support by funds provided by the Graduiertenkolleg "Die Erforschung subnuklearer Strukturen der Materie" is gratefully acknowledged.

Appendix A. Numerical method

In this appendix we briefly discuss the basis expansion of the Salpeter amplitudes and vertex functions for the numerical treatment of the Salpeter equation and the current matrix elements (see [6,7] for further details). Using the standard Dirac representation the Salpeter amplitude Φ is a 4×4 matrix in Dirac space, which can be written as a 2×2 block matrix of the form

$$\Phi = \begin{pmatrix} \Phi^{+-} & \Phi^{++} \\ \Phi^{--} & \Phi^{-+} \end{pmatrix}. \tag{A.1}$$

In the non-relativistic limit the Φ^{++} component can be identified with the ordinary Schrödinger wave function. Due to the special projector structure of the Salpeter equation, we find for the solutions

$$\Lambda_1^+(\mathbf{p})\Phi(\mathbf{p})\Lambda_2^+(-\mathbf{p}) = \Lambda_1^-(\mathbf{p})\Phi(\mathbf{p})\Lambda_2^-(-\mathbf{p}) = 0. \tag{A.2}$$

Thus, only two of these four amplitudes are independent, which allows to express Φ^{+-}, Φ^{-+} in terms of Φ^{++}, Φ^{--} by

$$\Phi^{+-} = +\frac{\omega_1}{m_2\omega_1 + m_1\omega_2}\Phi^{++}\sigma\mathbf{p} - \frac{\omega_2}{m_2\omega_1 + m_1\omega_2}\sigma\mathbf{p}\Phi^{--},$$

$$\Phi^{-+} = -\frac{\omega_1}{m_2\omega_1 + m_1\omega_2}\Phi^{--}\sigma\mathbf{p} + \frac{\omega_2}{m_2\omega_1 + m_1\omega_2}\sigma\mathbf{p}\Phi^{++}.$$

The amplitudes Φ^{++} and Φ^{--} can be decomposed in the general form

$$\Phi^{\pm\pm}_{J^{\pi\pi_c},M_J}(\mathbf{p}) = \sum_{L,S} \mathcal{R}^{(\pm)}_{LS}(p)\left[Y_L(\Omega_p) \times \varphi^{[S]}\right]_{JM_J}, \tag{A.3}$$

where $\varphi^{[0]} = \frac{1}{\sqrt{2}}\mathbb{1}$ and $\varphi^{[1]}_m = \frac{1}{\sqrt{2}}\sigma^{[1]}_m$ with $\sigma^{[1]}_m$ the spherical tensor components of the Pauli matrices. The sum runs over all combinations of spin S and angular momentum L coupled to J, which are compatible with the parity and C-parity of the state.

For the numerical solution of the Salpeter equation the radial amplitudes $\mathcal{R}^{(\pm)}_{LS}(p)$ are expanded in an L^2-orthonormal basis R_{nL} with

$$\mathcal{R}^{(\pm)}_{LS}(p) = \sum_n c^{(\pm)}_{nLS} R_{nL}(y),$$

where

$$R_{nL}(y) := N_{nL} y^L L_n^{2L+2}(y) e^{-y/2}, \tag{A.4}$$

$L_n^{2L+2}(y)$ being Laguerre polynomials in the argument $y = \beta p$, where the constant β sets the scale. The Salpeter equation is solved in this basis by taking up to 30 basis functions into account and using the variation principle with respect to the scale β. The resulting radial amplitudes $\mathcal{R}^{\pm}$ for the D, D^* and B mesons in model $\mathcal{A}$ and $\mathcal{B}$ are shown in figs. 7-9.

References

1. V. Ciulli, talk presented at the *8th International Symposium on Heavy Flavour Physics, University of Southampton, July 1999*, JHEP Conf. Proc. PRHEP-hf8/044, hep-ex/9911044.
2. M. Koll, R. Ricken, D. Merten, B. Metsch, H. Petry, Eur. Phys. J. A **9**, 73 (2000).
3. A. Kaufmann, diploma thesis, Universität Bonn, TK-99-01 (1999).
4. S. Godfrey, N. Isgur, Phys. Rev. D **32**, 189 (1985).
5. G. Zöller, S. Hainzl, C.R. Münz, M. Beyer, Z. Phys. C **68**, 103 (1995).
6. C.R. Münz, J. Resag, B.C. Metsch, H.R. Petry, Nucl. Phys. A **578**, 418 (1994).
7. J. Resag, C.R. Münz, B.C. Metsch, H.R. Petry, Nucl. Phys. A **578**, 379 (1994).
8. F. Gross, J. Milana, Phys. Rev. D **43**, 2401 (1991).
9. M. Böhm, H. Joos, M. Krammer, Nucl. Phys. B **51**, 397 (1973).
10. G. 't Hooft, Phys. Rev. D **14**, 3432 (1976).
11. M.A. Shifman, A.I. Vainshtein, V.I. Zakharov, Nucl. Phys. B **163**, 46 (1980).
12. R. Ricken, M. Koll, D. Merten, B. Metsch, H. Petry, Eur. Phys. J. A **9**, 221 (2000).
13. Particle Data Group (D.E. Groom *et al.*), Eur. Phy. J. C **15**, 1 (2000).
14. S. Mandelstam, Proc. R. Soc. **233**, 248 (1955).
15. Cleo Collaboration (S. Anderson *et al.*), Nucl. Phys. A **663-664**, 647 (2000).
16. J.D. Richman, P.R. Burchat, Rev. Mod. Phys. **67**, 893 (1995).
17. N. Isgur, M.B. Wise, Phys. Lett. B **232**, 113 (1989).
18. N. Isgur, M.B. Wise, Phys. Lett. B **237**, 527 (1990).
19. Cleo Collaboration (M. Athanas *et al.*), Phys. Rev. Lett. **79**, 2208 (1997).
20. D. Scora, N. Isgur, Phys. Rev. D **52**, 2783 (1995).
21. M. Wirbel, B. Stech, M. Bauer, Z. Phys. C **29**, 637 (1985).
22. D. Melikhov, B. Stech, hep-ph/0001113.
23. Cleo Collaboration (B. Barish *et al.*), Phys. Rev. D **51**, 1014 (1995).
24. Cleo Collaboration (J.P. Alexander *et al.*), hep-ex/0007052.
25. Opal Collaboration (G. Abbiendi *et al.*), Phys. Lett. B **482**, 15 (2000).
26. Belle Collaboration (K. Abe *et al.*), hep-ex/0111060, hep-ex/0111082.
27. Delphi Collaboration (P. Abreu *et al.*), Phys. Lett. B **510**, 55 (2001).
28. Cleo Collaboration (P. Avery *et al.*), CLEO CONF 94-7.
29. I. Caprini, L. Lellouch, M. Neubert, Nucl. Phys. B **530**, 153 (1998).
30. E791 Collaboration (E.M. Aitala *et al.*), Phys. Lett. B **440**, 435 (1998).
31. E791 Collaboration (E.M. Aitala *et al.*), Phys. Lett. B **450**, 294 (1999).
32. M. Neubert, B. Stech, in *Heavy Flavours II*, edited by A.J. Buras, M. Lindner (World Scientific, Singapore, 1998) p. 294.
33. M. Beneke, G. Buchalla, M. Neubert, C.T. Sachrajda, hep-ph/0006124.